Ultrasound assisted electrodeposition of Zn and Zn-TiO2 coatings

Camargo, MK, Tudela, I, Schmidt, U, Cobley, AJ & Bund, A

Original citation & hyperlink:
Camargo, MK, Tudela, I, Schmidt, U, Cobley, AJ & Bund, A 2016, 'Ultrasound assisted electrodeposition of Zn and Zn-TiO2 coatings' *Electrochimica Acta*, vol 198, pp. 287–295
https://dx.doi.org/10.1016/j.electacta.2016.03.078

DOI 10.1016/j.electacta.2016.03.078
ISSN 0013-4686

Publisher: Elsevier

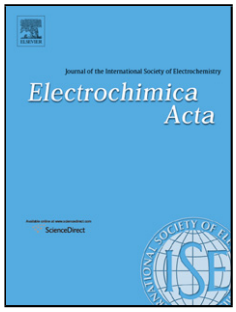

Title: Ultrasound assisted electrodeposition of Zn and Zn-TiO_2 coatings

Author: Magali K. Camargo Ignacio Tudela Udo Schmidt Andrew J. Cobley Andreas Bund

PII: S0013-4686(16)30618-1
DOI: http://dx.doi.org/doi:10.1016/j.electacta.2016.03.078
Reference: EA 26908

To appear in: *Electrochimica Acta*

Received date: 20-11-2015
Revised date: 9-3-2016
Accepted date: 12-3-2016

Please cite this article as: Magali K.Camargo, Ignacio Tudela, Udo Schmidt, Andrew J.Cobley, Andreas Bund, Ultrasound assisted electrodeposition of Zn and Zn-TiO2 coatings, Electrochimica Acta http://dx.doi.org/10.1016/j.electacta.2016.03.078

Ultrasound assisted electrodeposition of Zn and Zn-TiO_2 coatings

Magali K. Camargo[a*] magali.camargo@tu-ilmenau.de, Ignacio Tudela[b], Udo Schmidt[a], Andrew J. Cobley[b], Andreas Bund[a]

[a]Technische Universität Ilmenau, Electrochemistry and Electroplating Group, Gustav-Kirchhoff-Straße 6, 98693 Ilmenau, Germany

[b]The Functional Materials Applied Research Group, Faculty of Health and Life Sciences, Coventry University, Priory Street, CV15FB Coventry, United Kingdom

*Corresponding author.

Abstract

Pristine Zn and Zn-TiO_2 coatings were galvanostatically electrodeposited on steel substrates from additive-free chloride-based plating baths under silent and ultrasonic conditions. An ultrasonic bath-setup (38 kHz) was used as a sonoelectrochemical system. The influence of ultrasonic irradiation on the layer properties was investigated using different combinations of ultrasonic power and current density. In general, the use of ultrasonic irradiation for assisting the electrodeposition of pristine Zn and Zn-TiO_2 layers does have impact on the morphological and structural properties of the electrodeposits. The use of ultrasonic irradiation for dispersing particles during the electro-codeposition process was shown to be beneficial provided the use of suitable ultrasonic and deposition parameters. The incorporation of particles into the metallic matrix was confirmed with glow discharge optical emission spectroscopy investigations and focused-ion-beam-assisted cross-sectional analysis. The presence of TiO_2 agglomerates having smaller sizes as well as a better distribution in the metallic matrix was observed for the combination of ultrasonic agitation and high-speed electrodeposition. Pyramidal textures corresponding to the (101), (102), (103) and (112) planes were found characteristic for Zn layers having incorporated TiO_2 particles. One aspect of using ultrasonic agitation during electroplating is that Zn layers might also be prone to cavitation/erosion phenomena. Nevertheless, this effect can be controlled by adjusting the ultrasonic power as well as the ultrasonic irradiation time.

Keywords: ultrasound assisted electrodeposition; metal matrix composite coatings; particle incorporation; Zn-TiO2; GD-OES

1. Introduction

The development of functional coatings has promoted an extensive research of novel materials with potential applications for several high-tech areas. In this sense, metal matrix composites (MMC) can conveniently be produced via the electro-codeposition method [1]. The incorporation of a dispersed second phase material (e.g. micro/nano-particles) into the metal matrix during the electrodeposition process makes it possible to tune the properties of the MMC layers for a variety of applications. Since the industry of protective coatings demands environmentally friendly alternative materials, Zn-TiO_2 dispersion layers can be promising materials with enhanced properties such as hardness, wear and corrosion resistance. Furthermore, Zn-TiO_2 layers also acquire potential functionality as materials for water remediation technologies due to the photocatalytic properties of TiO_2 [2–4].

Generally, the successful achievement of composite layer properties is directly related to the amount of incorporated particles, their uniform distribution within the metal matrix as well as the resulting microstructure of the metal. According to the literature, the amount of incorporated metal oxide particles in Zn electrodeposits has generally been quite low. Some reported values for particle incorporation using diverse electrodeposition techniques can be mentioned as examples: TiO_2 up to 0.4 wt% by Alberts et al.[5], TiO_2 up to 0.42 wt.% by Frade et al.[6], ZrO_2 up to 0.4 wt.% by Vathsala et al.[7], SiO_2 up to 0.7 wt.% by Khan et al.[8] and SiO_2 up to 0.37 wt.% by Aslanidis et al.[9]. This demonstrates that the electro-co-deposition of metal oxides with Zn is challenging. In regard to this point, one obstacle for the incorporation of metal oxide particles via electro-codeposition processes is the low dispersion stability of metal oxide particles in plating baths due to the high ionic strength of such media [10,11]. Consequently, the agglomeration of particles in such media is difficult to avoid. Nevertheless, particle

agglomeration can be minimized and/or controlled by different dispersion methodologies (e.g. magnetic and mechanical stirring, wet ball milling, etc.) prior and/or during electrodeposition. In this regard, the use of ultrasonic irradiation can be a beneficial tool during the electro-codeposition process since ultrasound can promote the deagglomeration of particles and, consequently, the enhancement of the particle incorporation as well as their dispersion into the metal matrix.

The use of ultrasound in electrochemistry has been already reported for various applications such as environmental remediation, electro-organic synthesis, electroanalysis, production of nanomaterials as well as electrodeposition of metals and composites [12–14]. When ultrasound is introduced into an electrolyte, acoustic cavitation occurs. The resulting effects of ultrasound are different phenomena such as acoustic streaming, turbulent movement due to cavitation, micro-jetting and generation of shock waves [15]. These effects can promote favorable phenomena at the electrode/electrolyte interface such as the reduction of the diffusion layer thickness, the promotion of mass transport from/to the electrode and cleaning of the electrode surface [13,15,16]. Consequently, advantages such as increased deposition rates, reduced porosity and grain refinement have been reported for ultrasound-assisted electroplating [13,17]. Some works on ultrasound assisted electrodeposition of coatings have reported the improvement of structural and mechanical layer properties as well [14,18,19].

This work presents a comparative study of the influence of ultrasound on the electrodeposition of pristine Zn as well as Zn-TiO_2 composite layers from additive-free chloride-based electrolytes. An ultrasonic bath (US-bath) was used as a sonoelectrochemical system to study the use of 38 kHz ultrasonic frequency in combination with different ultrasonic power densities during electrodeposition. The particle co-deposition as well as the morphological, structural and mechanical properties

of the layers were investigated and correlated with the ultrasonic as well as the electroplating parameters.

2. Experimental part

2.1 Ultrasound-assisted electrodeposition

Table 1 describes the chemical composition of the plating bath as well as the electrodeposition parameters. The electroplating bath was prepared using reagent grade chemicals and deionized water. TiO_2 nano-particles (TiO_2 P25, average primary size 21 nm, Evonik GmbH) were used as received.

The ultrasonic irradiation was provided by an ultrasonic bath (frequency: 38 kHz, maximum nominal power: 200 W, Ultrawave QS12). **Figure 1** shows the schematic representation of the US-bath setup used in this investigation. It consisted of a plating cell with a rotating disk electrode (RDE) immersed in the ultrasonic bath. A cylindrical glass vessel containing 580 mL of electrolyte was used as a cell. The cathode and anode were positioned as shown in **Figure 1**, the distance between electrodes was 2.0 cm. The use of the RDE together with the US-bath was necessary because of two reasons. First, the agitation provided by the US-bath on its own was not enough to accomplish the deposition of homogeneous Zn layers. It is important to remark that acidic chloride-based zinc electrolytes are characterized by high exchange currents. Consequently either dendritic or powdery deposits are expected if plating additives and/or suitable hydrodynamic control are not in use [20]. On the other hand, the use of US-bath agitation on its own did not avoid the partial sedimentation of particles during deposition. Therefore, a RDE was introduced to the system in order to assist a uniform dispersion of particles as well as to establish well-defined hydrodynamic conditions. The rotation speed was kept constant to 600 rpm for all experiments.

Prior to electrodeposition the steel substrates were degreased with acetone, rinsed in distilled water, pickled in HCl (1:1 v/v) solution for 15 seconds and finally rinsed again in distilled water. Pristine Zn and Zn-TiO_2 layers were electrodeposited galvanostatically at 2, 4, 6, 10 and 20 A/dm^2. Different combinations of ultrasonic power densities and deposition current densities were studied. Furthermore, control tests under silent conditions were performed. A cooling system was necessary to keep the temperature during deposition constant. It consisted of a coiled copper tube connected to a Julabo-FL300 recirculating cooling system. The temperature was kept at 21 ± 1°C during the electrodeposition experiments. After electrodeposition, the samples and ultrasonically cleaned in distilled water for 2 min (38 kHz, maximum power) in order to clean any non-incorporated TiO_2 particles attached to the surface of the deposit.

The ultrasonic power delivered to the electrochemical system was determined by calorimetry (for this purpose the cooling of the system was turned off). The temperature (T) of the electrochemical cell containing 580 mL of deionized water was recorded against the time (t) every 15 s after the initiation of sonication. A thermocouple with the sensor located in the central part of the cell was used. The total time for data recording was 2 minutes. From the T *versus* t data, dT/dt can be estimated by constructing a tangent to the curve at t=0. The initial temperature rise induced by ultrasound can be converted into energy input; in this way, the ultrasonic power (in W) is calculated from **Eq.(1)** [21].

$$Power = mC_p(dT/dt) \qquad \textbf{(1)}$$

Where *m* is the mass of water in the cell (kg), C_p is the specific heat of water ($Jkg^{-1}K^{-1}$) at constant pressure and *dT/dt* (Ks^{-1}) is the slope of the temperature curve at t=0.

2.2 Characterization of the layers

The surface morphology of the deposits was studied using a Hitachi S4800 scanning electron microscope (SEM). The SEM observations were performed at the central area of

the samples. The topography and roughness of the layers were examined using a laser profilometer (UBM, type UBC 14, UBM Messtechnik GmbH). Depth profile analyses were performed by glow-discharge optical emission spectroscopy (GD-OES) at the central part of samples in order to study particle incorporation. For this purpose, a GDA 750 spectrometer (Spectruma Analytic GmbH) equipped with a DC source (1000 V, 13 mA) was used. The inner diameter of the anode (exposed sample) was 4 mm. Furthermore, the coating thickness and the elemental composition of the layers were studied by X-ray fluorescence (XRF) (FISCHERSCOPE®X-rayXDV®-SDD). Cross-sectional studies of the layers were conducted using a Carl Zeiss AURIGA 60 Cross Beam Workstation (FIB).

Microstructural investigations were performed using X-ray diffraction (XRD). An X-ray diffractometer Bruker AXS D 5000 operating with Cu-Kα radiation and Bragg Brentano geometry was used. The diffraction patterns were recorded with a step size of 0.02° for 2θ ranging from 20° to 100° and a measuring time of 1.4 s per step. The sample area of analysis was approx. 1 cm^2. In order to describe the structure and to quantitatively estimate the preferred orientation of the Zn deposits, the relative texture coefficient $RTC_{(hkl)}$ was calculated from **Eq. (2)** [22,23]:

$$\mathbf{RTC_{(hkl)}} = \frac{\mathbf{I_{hkl}/I^{\circ}_{hkl}}}{\sum_1^8 \mathbf{I_{hkl}/I^{\circ}_{hkl}}} \times \mathbf{100}\% \qquad \mathbf{(2)}$$

In **Eq. (2)** I_{hkl} corresponds to the diffraction intensities of the (hkl) lines measured in the diffraction pattern of the deposit and $I°_{hkl}$ are the corresponding intensities of a standard Zn powder sample with random orientation [24]. The summation in the denominator is taken for the first eight diffraction peaks ((002), (100), (101), (102), (103), (110), (004) and (112)) that are visible in the XRD pattern. A plane having a RTC value higher than 12.5 % (100/8 %) was considered as preferred.

Universal hardness measurements were performed in the cross-section of the layers using a HM500 Fischer picoindentor. To measure the hardness in the layer's cross-section, the deposits were plated using twice the usual deposition time. A 25 mN load was applied during 30 s for each measurement. Ten indentations per sample were carried out. The conversion from Universal hardness units into Vickers hardness units was performed based on the DIN EN ISO 14577-1 norm, attachment F. The sample preparation included the embedding of the layers in epoxy resin followed by a step-by-step grinding with SiC paper. The final polishing was performed using 0.05 µm Al_2O_3 ethanolic suspension. Afterwards, the samples were ultrasonically cleaned in isopropanol media and dried.

3. Results and discussion

3.1 Ultrasonic power measurement

The ultrasonic power applied to the electrochemical system (US-bath setup) was determined by calorimetric methodology (**Eq.(1)**) [21]. The calorimetric determined ultrasonic power can be divided by the total amount of electrolyte (580 mL) to obtain the ultrasonic power density. **Table 2** shows the ultrasonic power input values given as ultrasonic power density (in W/cm^3).

3.2 Effect of ultrasound on the surface morphology

Pristine Zn layers:

As a first approach, the influence of sonication during the electrodeposition of pristine Zn was investigated. In general, it is known that Zn layers deposited from additive-free chloride-based plating baths under silent conditions produce coarse-grained deposits having irregular morphology particularly at low current densities [20,25].

Figure 2 depicts the effect of 38 kHz ultrasonic irradiation on the morphology of Zn deposits plated at low current density (2 A/dm^2). It can be seen that the ultrasonic irradiation provided by the US-bath promoted a leveling effect during Zn

electrodeposition. The surface of the deposit plated under 53 mW/cm^3 power density (**Figure 2c**) ultrasound irradiation exhibited a smoother morphology ($R_a \approx 1.5$ μm) compared to the deposits obtained under 28 mW/cm^3 power density (**Figure 2b**) and silent conditions (**Figure 2a**) ($R_a \approx 2.5$ μm in both cases). At deposition rates higher than 2 A/dm^2 the leveling effect of ultrasound progressively diminished since the total amount of ultrasonic energy provided to the cell as well as the number of cavitation events decreased. Consequently, at 20 A/dm^2 the influence of ultrasound irradiation on the deposit's roughness was negligible.

Zn-TiO_2 composite layers:

Zn-TiO_2 composite layers with significant differences in their structural and morphological characteristics were obtained by varying both the ultrasonic power density and the deposition current density. It was found that surface erosion took place when current densities lower than 20 A/dm^2 were applied. On the other hand, the particular use of 6 A/dm^2 in combination with 53 mW/cm^3 resulted in the patterning of the layer surface. As displayed in **Figure 3a**, this layer exhibited a patterned morphology consisting of nodular structures uniformly distributed over the whole surface. These morphological characteristics were not observed at all in similar ultrasound-assisted experiments for pristine Zn. Likewise, the patterning of the layer was not observed for Zn-TiO_2 deposits plated under silent conditions. Therefore, these observations suggests that the presence of particles in the electrolyte in combination with the ultrasonic irradiation led to the obtention of a more heterogeneous surface finishing consisting in nodular structures. This effect might be attributed to the collapse of cavitation bubbles and the subsequent formation of strong microjets of electrolyte containing particles. Besides the fact that particles can participate in the co-deposition process, they might also violently hit the growing Zn layer. Consequently, the use of ultrasonic irradiation can

lead to the development of heterogeneous Zn-TiO_2 layers especially when low current densities (which results on long irradiation times) are applied. Only the use of the highest deposition rate of 20 A/dm^2 (which implies a short irradiation time) in combination with 53 mW/cm^3 led to a homogeneous composite layer with a smooth surface finish (**Figure 3b**). In this case, the quick growth of the layer hindered the effect explained previously.

Figure 4 shows the SEM micrographs of the Zn-TiO_2 layers deposited using high speed deposition at 20 A/dm^2 (shortest irradiation time) under silent conditions (**Figure 4a**) as well as under 28 mW/cm^3 (**Figure 4b**) and 53 mW/cm^3 (**Figure 4c**) ultrasonic power densities. It can be seen that all layers exhibited similar morphologies. However, whereas deposition under silent conditions yielded a porous layer, ultrasound assisted deposition promoted layers with higher compactness. This can be ascribed to the effect of the ultrasound assisting the removal of H_2 that might be produced at the cathode during the electrodeposition, especially at such fast deposition rate. Furthermore, ultrasound assists in controlling/improving the dispersion stability of TiO_2 in the media and, consequently, can contribute to the development of layers with enhanced compactness. Although, changes in the microstructure of the layers might also contribute to the enhancement of compactness in this specific case, microstructural changes due to ultrasound were not observed. This observation is discussed in **Section 3.4** of this paper in more detail.

3.3 Effect of ultrasound on TiO_2 particle incorporation

The effect of ultrasound on the co-deposition of TiO_2 with Zn was studied on layers plated with different combinations of electrochemical and ultrasonic parameters. Provided the sample exhibited a relatively homogeneous and even surface, the amount of incorporated TiO_2 was studied by GD-OES. For the other cases (layers with high levels of roughness or uneven surfaces) XRF methodology was used. In contrast to GD-OES (which provides a depth profile analysis), XRF provides only an averaged value of the

particle content in the layer.

Figure 5 shows the depth profile analyses of Zn-TiO_2 layers plated at 20 A/dm^2 under both silent and ultrasonic irradiation conditions. The concentration of TiO_2, Zn and Fe is plotted against the thickness of the layers. The concentration of TiO_2 was calculated stoichiometrically based on the Ti concentration. Under silent conditions, the incorporation of TiO_2 across the whole thickness of Zn the layer can be observed. The particle concentration was higher both at the Zn/substrate interface and at the Zn surface in comparison to the bulk zone of the layer. Under 28 mW/cm^3 ultrasonic power density, the concentration of TiO_2 became more homogeneous across the layer thickness despite that the overall amount of TiO_2 seemed to be slightly lower than that of the deposits produced under silent conditions. On the other hand, the use of 53 mW/cm^3 ultrasonic power density led to an enhancement of particle incorporation as well as a uniform TiO_2 content across the thickness of the layer. It is noteworthy mentioning that the layers plated in the presence of ultrasound did not exhibit a high concentration of TiO_2 at the deposit´s plain surface. Therefore, the presence of a relative high TiO_2 amount at the layer surface deposited under silent conditions is only due to adsorption (and not embedding) of TiO_2 particles [10,26].

Under silent conditions, a decrease in co-deposition was observed as the deposition time gets longer. This can be ascribed to the variation of TiO_2 agglomerate sizes with the deposition time. At early stages of deposition, the particles are fresh dispersed and, therefore, a higher co-deposition of particles might take place. As the deposition time went on the particles tended to agglomerate and, consequently, the amount of well-dispersed ‘effective’ particles for co-deposition decreased [27].

Figure 6 shows the average particle incorporation for layers obtained at different current densities. Due to the heterogeneous surface morphologies of the layers plated under

ultrasonic irradiation at deposition rates lower than 20 A/dm^2, the particle content in those cases was determined by XRF methodology. In the other cases (layers plated at 20 A/dm^2) GD-OES analysis was possible and the TiO_2 average content was calculated from the depth profile zone situated between 2 µm and 7 µm of the coating thickness. The co-deposition of TiO_2 was possible in the whole current density range of study. At 20 A/dm^2, the particle incorporation was enhanced by 35% due to the use of ultrasound-assisted plating. On the other hand, XRF studies confirmed co-deposition of TiO_2 in the layers deposited under ultrasonic irradiation at current densities lower than 20 A/dm^2 but, due to the higher uncertainty of XRF, it was not possible to confirm any ultrasound related enhancement of particle incorporation.

FIB assisted cross sectional SEM micrographs from layers electroplated at 20 A/dm^2 under silent as well as under 53 mW/cm^3 ultrasonic power density are displayed in **Figure 7**. It has been reported that materials having hexagonal crystallographic structure such as Zn are prone to develop artifacts such as 'curtain effects' and material re-deposition (formation of protuberances at some zones of the material) during ion-beam milling [28,29]. In this case, despite the use of protective Pt layers (to minimize any damage to the layer during the ion-beam milling process), it was not possible to avoid at all those artifacts. Nevertheless, the presence of TiO_2 particles (detected as 'dark spots' with EsB and EDX detectors on FIB analysis area) could be distinguished from the Zn metal matrix. In the case of silent electrodeposition (**Figure 7a**), the incorporation of TiO_2 can be observed as a relatively small number of particle agglomerates poorly distributed within the Zn matrix. Whereas, the layer deposited under ultrasonic conditions (**Figure 7b)** contained quite well-distributed particle agglomerates. This confirms that the use of ultrasound promoted the uniform distribution of particles during the co-deposition process. It is noteworthy to mention that the size of the incorporated TiO_2 agglomerates

was generally not bigger than approx. 200 nm in both layers. However, when ultrasonic agitation was used, a more consistent presence of smaller agglomerates could be seen. Similar results for other different electrodeposited composite layers were also reported in the literature [12,17,19].

3.4 Effect of ultrasound on the microstructure and texture

The influence of the ultrasound irradiation as well as the incorporation of TiO_2 particles on the developed structure of Zn was investigated by XRD methodology. The diffraction peaks from the XRD patterns (not shown) of the layers correspond to the hexagonal structure of Zn. The findings from XRD characterization of the deposits are discussed in terms of the relative texture coefficients (RTCs). The first eight diffraction peaks corresponding to: i) the basal planes: (002) and (004), ii) the prism planes: (100) and (110) and, iii) the pyramidal planes: (101), (102), (103) and (112) were considered for the RTC calculation.

Figure 8a displays the RTC values of the pristine Zn layers produced at 2 A/dm^2 under silent conditions and ultrasonic irradiation. The horizontal red dashed line indicates the minimum RTC value (12.5%) that any RTC must exceed in order to be considered as preferred. One can see that under silent conditions the pyramidal (110) and (112) textures are preferred. These observations are in agreement with studies on Zn layers from additive-free chloride electrolytes carried out by Mouanga et al. [30]. It can be seen as well that most of the 'non-preferred' RTCs actually presented a considerable contribution to the layer texture. Therefore, this layer can be roughly considered as randomly oriented. When 28 mW/cm^3 ultrasonic power density was employed, the layer developed a stronger (112) pyramidal texture. Under 53 mW/cm^3, the RTC value of the basal plane (002) increased considerably and became preferred together with the pyramidal (103) texture. Those changes can firstly be ascribed to changes in the electrocrystallization

process of Zn influenced by ultrasound. However, the deformation of the Zn surface due to cavitation and erosion phenomena might also contribute to those microstructural changes [31,32].

Figure 8b shows that no significant changes in the layers' texture were found for the pristine layers plated at the lowest irradiation time (20 A/dm^2). Due to the high deposition rate, the total energy supplied by ultrasound was not enough to produce significant variations in the texture. By comparing **Figure 8b** and **Figure 8c**, it can be seen the effect of particles on the resulting texture of Zn-TiO_2 layers in the presence and the absence of ultrasonic agitation at 20 A/dm^2. All composite layers show as common feature the diminishment of RTC value of basal plane (002) as well as the increase of the pyramidal (102) and (103) textures. Those changes in structure can be ascribed to the incorporation of particles into the Zn layer, the presence of particles in the plating bath or, most likely, to the combination of both. Either way, it is clear that the presence of particles in the process promotes changes in the texture. The predominant textures found in the composite layers were the (102) and (103). This suggests that the particle incorporation is likely to occur when Zn crystallite growth involves pyramidal textures. Furthermore, similarly to the case of pristine Zn layers, the use of ultrasound at such high deposition rates did not cause any significant change in the microstructure of the composite layers.

In general, the results suggest that the growth of Zn in a direction to pyramidal planes can be correlated to the probability that a particle remains on the electrode during the metal electrodeposition and, therefore, with particle incorporation. Similar results were found in previous work for Zn-TiO_2 layers deposited under silent conditions from additive-free chloride- and sulfate-based plating baths at pH 5.3 [10] as well as for Zn-TiO_2 composite layers prepared from sulfate-based baths at pH 4 using pulse plating deposition [33]. **Figure 9** shows a schematic representation of different developed textures for Zn during

deposition. It can be seen that pyramidal textures can promote a growing of less ordered Zn platelets, those imperfections might increase the probability that particles remain on the electrode and become embedded during metal deposition.

3.5 Effect of ultrasound on the hardness of deposits

The influence of ultrasonic irradiation on the hardness of pristine as well as composite layers plated under different deposition conditions was investigated.

Figure 10 shows the hardness of deposits obtained under silent conditions as well as under 38 kHz ultrasonic irradiation. In general, it can be seen that the hardness of all pristine Zn layers fluctuated between 34 and 44 HV. No significant changes were found between silent and ultrasonic conditions, as the standard deviations for these measurements were not negligible. On the other hand, the composite Zn-TiO_2 layers plated at 20 A/dm^2 under 28 and 53 mW/cm^3 ultrasonic power densities exhibited an enhancement of hardness (up to ~56 HV in both cases) in comparison to the layer plated at silent conditions. This increase in hardness can be ascribed to the higher compactness (**Figure 4**) as well as the higher amount and the better distribution of incorporated TiO_2 observed in these deposits (**Figure 5**). In this specific case, the influence of the matrix microstructure on the coating's hardness could be neglected since all deposits obtained at 20 A/dm^2 exhibited a very similar texture (**Figure 8c**).

4. Conclusions/summary

The influence of 38 kHz ultrasonic irradiation (US-bath setup) on the electrodeposition of Zn and Zn-TiO_2 composite layers has been studied using additive-free chloride-based electrolytes. It was shown that ultrasonic irradiation can significantly change the morphological and structural properties of Zn and Zn-TiO_2 electrodeposits. By combining ultrasonic irradiation and high-speed deposition, compact and homogeneous Zn-TiO_2

layers with enhanced particle incorporation, better particle distribution in the matrix as well as improved hardness were obtained. Pyramidal textures were found to be characteristic for the Zn layers having incorporated TiO_2 particles. These observations suggests that the particle agglomerates, in sub-micro scale range according to FIB-assisted cross sectional observations, might get more easily stacked in between Zn platelets having pyramidal textures during electrodeposition.

Furthermore, the preparation of surface patterned Zn-TiO_2 layers (with higher surface area) was possible using a specific combination of ultrasonic and electrodeposition parameters. Another important aspect to consider is that Zn layers might be prone to surface erosion due to ultrasonic cavitation phenomena. The use of long irradiation times (which implies the use of low current densities) as well as the presence of particles in the plating bath might enhance surface erosion of the layers.

Generally, it was demonstrated that ultrasonic agitation does have an impact on the electrodeposition of Zn and Zn-TiO_2. Therefore, it can be a beneficial tool for tuning Zn electrodeposits properties depending on its potential application/functionality. The fundamental understanding of the processes involved must be improved by further research before an exploitation in technical processes becomes possible.

5. Acknowledgements

M.C. gratefully thanks the German Academic Exchange Service (DAAD) for the financial support through a doctoral grant. M.C. is also grateful to Dr. Graves for the support during the research stay at Coventry University. The support of Dr. Ispas and funding of Gleichstellungsrat-TU Ilmenau for making possible the research stay is also acknowledged. The authors thank Mr. Wilke and Mrs. Roßberg for GD-OES measurements and FIB assisted cross-sectional micrographs respectively. Helpful discussions with Dr. Grieseler and Dr. Kups concerning XRD data are also acknowledged.

References

[1] A. Hovestad, L.J.J. Janssen, Electrochemical codeposition of inert particles in a metallic matrix, J. Appl. Electrochem. 25 (1995) 519–527. doi:10.1007/BF00573209.

[2] S. Ito, T. Deguchi, K. Imai, M. Iwasaki, H. Tada, Preparation of Highly Photocatalytic Nanocomposite Films Consisting of TiO 2 Particles and Zn Electrodeposited on Steel, Electrochem. Solid-State Lett. 2 (1999) 440–442.

[3] T. Deguchi, K. Imai, H. Matsui, M. Iwasaki, H. Tada, S. Ito, Rapid electroplating of photocatalytically highly active TiO 2 -Zn nanocomposite films on steel, J. Mater. Sci. 36 (2001) 4723–4729.

[4] T. Frade, M.E. Melo Jorge, A. Gomes, One-dimensional ZnO nanostructured films: Effect of oxide nanoparticles, Mater. Lett. 82 (2012) 13–15. doi:10.1016/j.matlet.2012.05.028.

[5] D. Alberts, B. Fernández, T. Frade, A. Gomes, M.I.D.S. Pereira, R. Pereiro, et al., Depth profile characterization of Zn-TiO2 nanocomposite films by pulsed radiofrequency glow discharge-optical emission spectrometry., Talanta. 84 (2011) 572–8. doi:10.1016/j.talanta.2011.01.076.

[6] T. Frade, V. Bouzon, A. Gomes, M.I. da Silva Pereira, Pulsed-reverse current electrodeposition of Zn and Zn-TiO2 nanocomposite films, Surf. Coat. Technol. 204 (2010) 3592–3598. doi:10.1016/j.surfcoat.2010.04.030.

[7] K. Vathsala, T.V. Venkatesha, Zn–ZrO2 nanocomposite coatings: Elecrodeposition and evaluation of corrosion resistance, Appl. Surf. Sci. 257 (2011) 8929–8936. doi:10.1016/j.apsusc.2011.05.067.

[8] T.R. Khan, A. Erbe, M. Auinger, F. Marlow, M. Rohwerder, Electrodeposition of zinc–silica composite coatings: challenges in incorporating functionalized silica particles into a zinc matrix, Sci. Technol. Adv. Mater. 12 (2011) 055005. doi:10.1088/1468-6996/12/5/055005.

[9] D. Aslanidis, J. Fransaer, J.P. Celis, The Electrolytic Codeposition of Silica and Titania Modified Silica with Zinc, J. Electrochem. Soc. 144 (1997) 2352–2357.

[10] M.K. Camargo, U. Schmidt, R. Grieseler, M. Wilke, A. Bund, Electrodeposition of Zn-TiO2 Dispersion Coatings: Study of Particle Incorporation in Chloride and Sulfate Baths, J. Electrochem. Soc. 161 (2014) D168–D175. doi:10.1149/2.066404jes.

[11] A. Bund, D. Thiemig, Influence of bath composition and pH on the electrocodeposition of alumina nanoparticles and copper, J. Appl. Electrochem. 37 (2007) 345–351. doi:10.1007/s10800-006-9264-2.

[12] I. Tudela, Y. Zhang, M. Pal, I. Kerr, A.J. Cobley, Ultrasound-assisted electrodeposition of composite coatings with particles, Surf. Coatings Technol. 259 (2014) 363–373. doi:10.1016/j.surfcoat.2014.06.023.

[13] B.G. Pollet, Power Ultrasound in Electrochemistry: From Versatile Laboratory Tool to Engineering Solution, John Wiley & Sons, Ltd, Chichester, 2012. doi:10.1002/9781119967392.index.

[14] P. Sakkas, O. Schneider, S. Martens, P. Thanou, G. Sourkouni, C. Argirusis, Fundamental studies of sonoelectrochemical nanomaterials preparation, J. Appl. Electrochem. 42 (2012) 763–777. doi:10.1007/s10800-012-0443-z.

[15] J. Klima, Application of ultrasound in electrochemistry. An overview of mechanisms and design of experimental arrangement., Ultrasonics. 51 (2011) 202–9. doi:10.1016/j.ultras.2010.08.004.

[16] J. Louisnard, O., González-García, Acoustic cavitation, in: J. (Eds. . Feng, H., Barbosa-Canovas, G., Weiss (Ed.), Ultrasound Technol. Food Bioprocess., Springer, New York, 2011.

[17] E. García-Lecina, I. García-Urrutia, J. a. Díez, J. Morgiel, P. Indyka, A comparative study of the effect of mechanical and ultrasound agitation on the properties of electrodeposited Ni/Al2O3 nanocomposite coatings, Surf. Coatings Technol. 206 (2012) 2998–3005. doi:10.1016/j.surfcoat.2011.12.037.

[18] E. García-Lecina, I. García-Urrutia, J.A. Díez, J. Fornell, E. Pellicer, J. Sort, Codeposition of inorganic fullerene-like WS2 nanoparticles in an electrodeposited nickel matrix under the influence of ultrasonic agitation, Electrochim. Acta. 114 (2013) 859–867. doi:10.1016/j.electacta.2013.04.088.

[19] D. Dietrich, I. Scharf, D. Nickel, L. Shi, T. Grund, T. Lampke, Ultrasound technique as a tool for high-rate incorporation of Al2O3 in NiCo layers, J. Solid State Electrochem. 15 (2011) 1041–1048. doi:10.1007/s10008-011-1348-1.

[20] R. Winand, Electrodeposition of zinc and zinc alloys, in: Mordechay Schlesinger, M. Paunovic (Eds.), Mod. Electroplat., John Wiley & Sons, Inc., 2010: pp. 285–307.

[21] T.J. Mason, J.P. Lorimer, D.M. Bates, Quantifying sonochemistry: casting some light on a "black art," Ultrasonics. 30 (1992) 40–42.

[22] L.P. Bérubé, G. L'Espérance, A Quantitative Method of Determining the Degree of Texture of Zinc Electrodeposits, J. Electrochem. Soc. 136 (1989) 2314–2315. doi:10.1149/1.2097318.

[23] S. Spanou, E. a. Pavlatou, N. Spyrellis, Ni/nano-TiO2 composite electrodeposits: Textural and structural modifications, Electrochim. Acta. 54 (2009) 2547–2555. doi:10.1016/j.electacta.2008.06.068.

[24] JCPDS-ICDD: powder diffraction files Zn 04-0831. PN: International Center for Diffraction Data; Bd Sets 1–50, 70–88. PDF-3. Newtown Square 2000, PN: International Centre for Diffraction Data, n.d.

[25] T. Watanabe, Nano-Plating, 1st ed., Elsevier, Oxford, 2004.

[26] M. Camargo, I. Diaz, U. Schmidt, A. Bund, I. Díaz, U. Schmidt, et al., Synthesis, characterization and corrosion resistance of electroless Ni-P and Ni-P-SiC coatings: A comparative study, Galvanotechnik. 103 (2012) 48–56.

[27] S.L. Kuo, Y.C. Chen, M. Der Ger, W.H. Hwu, Nano-particles dispersion effect on Ni/Al2O3 composite coatings, Mater. Chem. Phys. 86 (2004) 5–10. doi:10.1016/j.matchemphys.2003.11.040.

[28] B.I. Prenitzer, C. a Urbanik-Shannon, L. a Giannuzzi, S.R. Brown, R.B. Irwin, T.L. Shofner, et al., The correlation between ion beam/material interactions and practical FIB specimen preparation., Microsc. Microanal. 9 (2003) 216–236. doi:10.1017/S1431927603030034.

[29] J. Li, Advanced Techniques in TEM Specimen Preparation, in: Khan Maaz (Ed.), Transm. Electron Microsc., InTech, 2012: pp. 69–84.

[30] M. Mouanga, L. Ricq, J. Douglade, P. Berçot, Effects of some additives on the corrosion behaviour and preferred orientations of zinc obtained by continuous current deposition, J. Appl. Electrochem. 37 (2007) 283–289. doi:10.1007/s10800-006-9255-3.

[31] S. Verdan, G. Burato, M. Comet, L. Reinert, H. Fuzellier, Structural changes of metallic surfaces induced by ultrasound., Ultrason. Sonochem. 10 (2003) 291–5. doi:10.1016/S1350-4177(03)00106-8.

[32] a. Chiba, W.C. Wu, Surface morphology of electrodeposited zinc films from zinc chloride solution under hydrostatic pressures, J. Mater. Sci. Lett. 12 (1993) 1266–1267. doi:10.1007/BF00506332.

[33] A. Gomes, M.I. Pereira, M.H. Mendonça, F.M. Costa, Zn–TiO2 composite films prepared by pulsed electrodeposition, J. Solid State Electrochem. 9 (2004) 190–196. doi:10.1007/s10008-004-0573-2.

Figure Captions

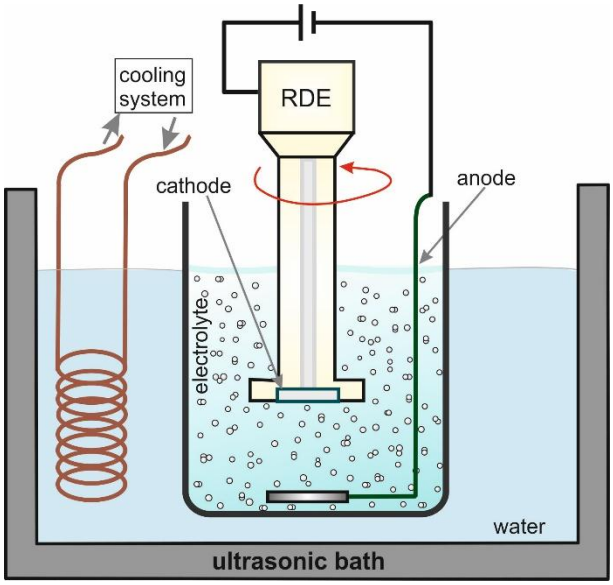

Figure 1 Schematic representation of the ultrasonic-bath (US-bath) setup for ultrasound-assisted electrodeposition experiments.

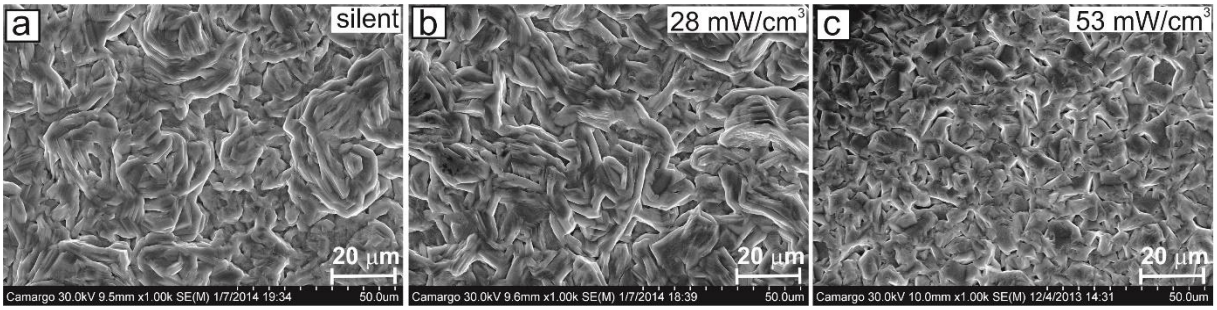

Figure 2 Influence of 38 kHz ultrasonic irradiation (US-bath setup) on the surface morphology of Zn electrodeposits plated at 2 A/dm^2: a) silent conditions b) under 28 mW/cm^3 and c) under 53 mW/cm^3 ultrasonic power density.

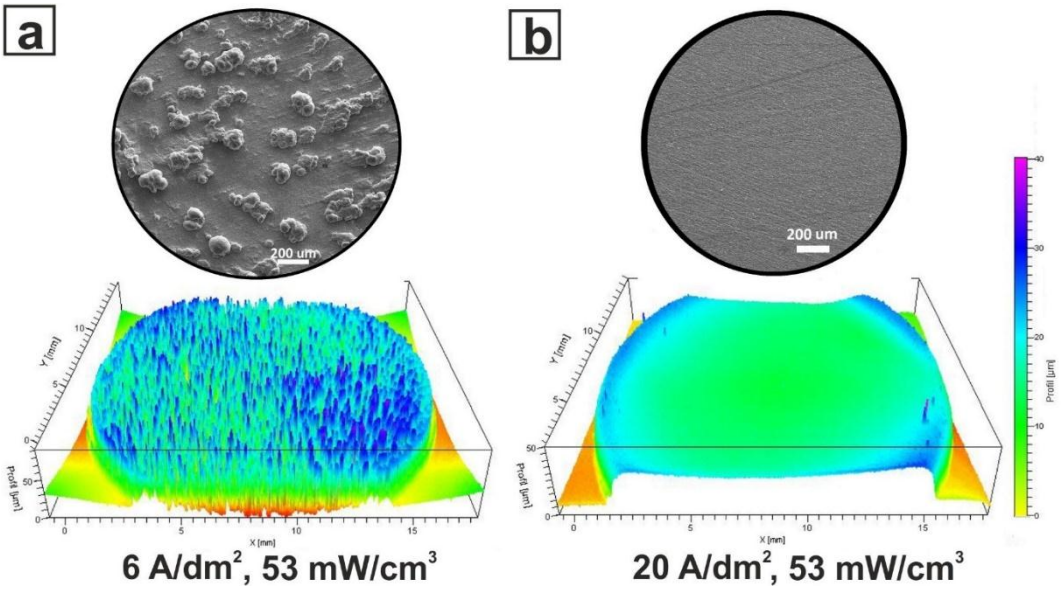

Figure 3 Surface morphology (up) and surface topography (down) of Zn-TiO_2 layers plated under 53 mW/cm^3 ultrasonic power density (US-bath setup) at: a) 6 A/dm^2 and b) 20 A/dm^2.

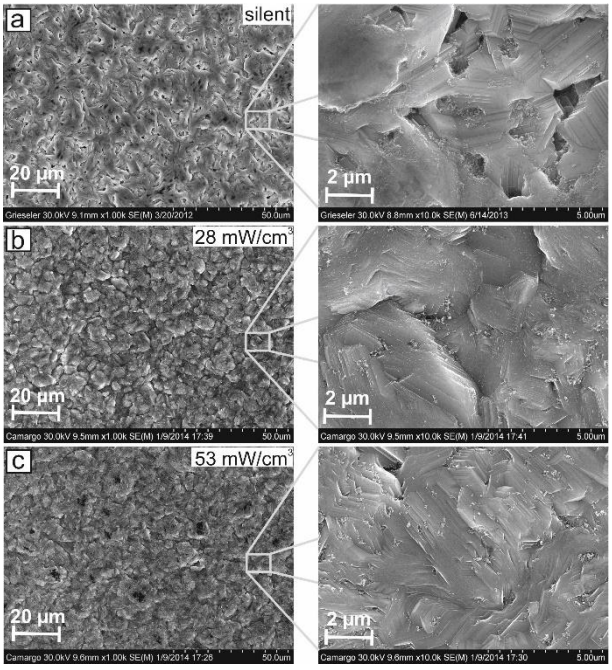

Figure 4 Influence of 38 kHz ultrasonic irradiation (US-bath setup) on the surface morphology of Zn-TiO_2 electrodeposits plated at 20 A/dm^2: a) silent conditions, b) under 28 mW/cm^3 and c) under 53 mW/cm^3 ultrasonic power density.

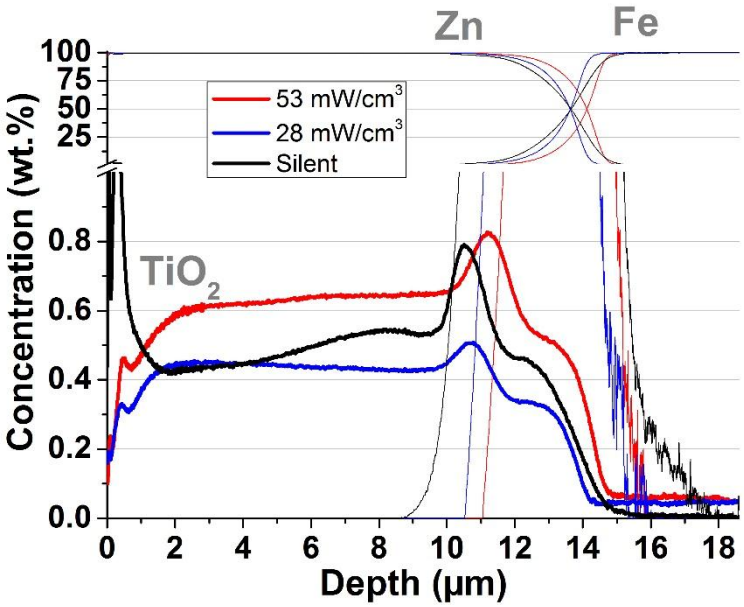

Figure 5 Depth profile analysis by GD-OES of Zn-TiO_2 layers plated at 20 A/dm^2 under silent conditions as well as under 28 mW/cm^3 and 53 mW ultrasonic power densities (US-bath setup).TiO_2 concentration in the plating bath: 15 g/L.

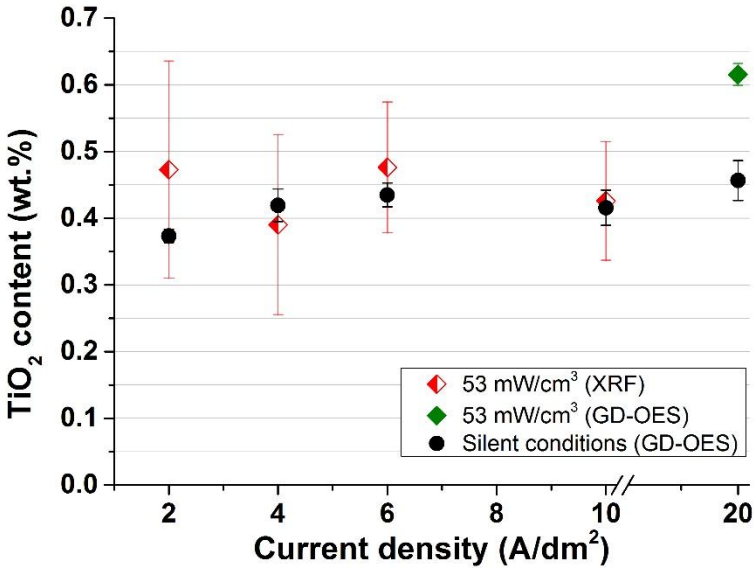

Figure 6 TiO_2 content (wt.%) in Zn-TiO_2 layers plated at different current densities under silent as well as under 53 mW/cm^3 ultrasonic power density (US-bath setup).

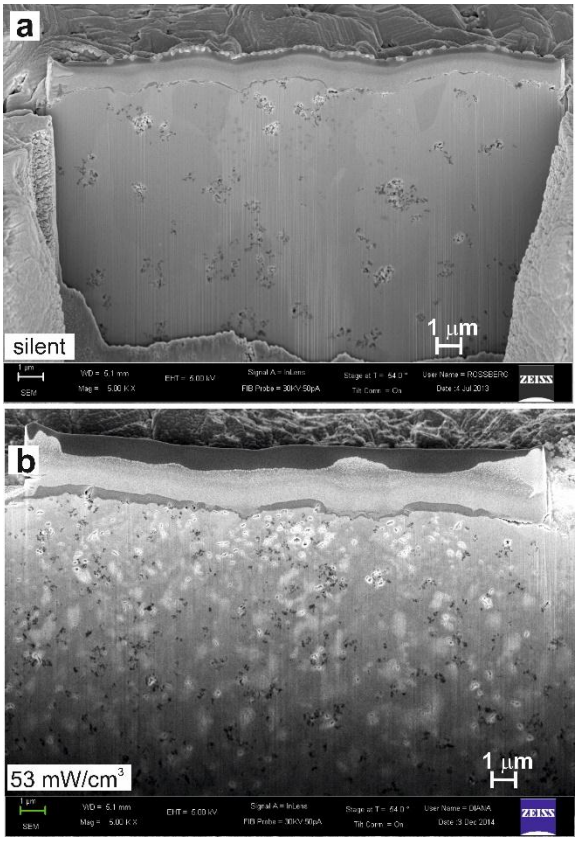

Figure 7 FIB-assisted cross sectional view of Zn-TiO_2 layers plated at 20 A/dm^2 under: a) silent conditions and b) 53 mW/cm^3 ultrasonic power density (US-bath setup).

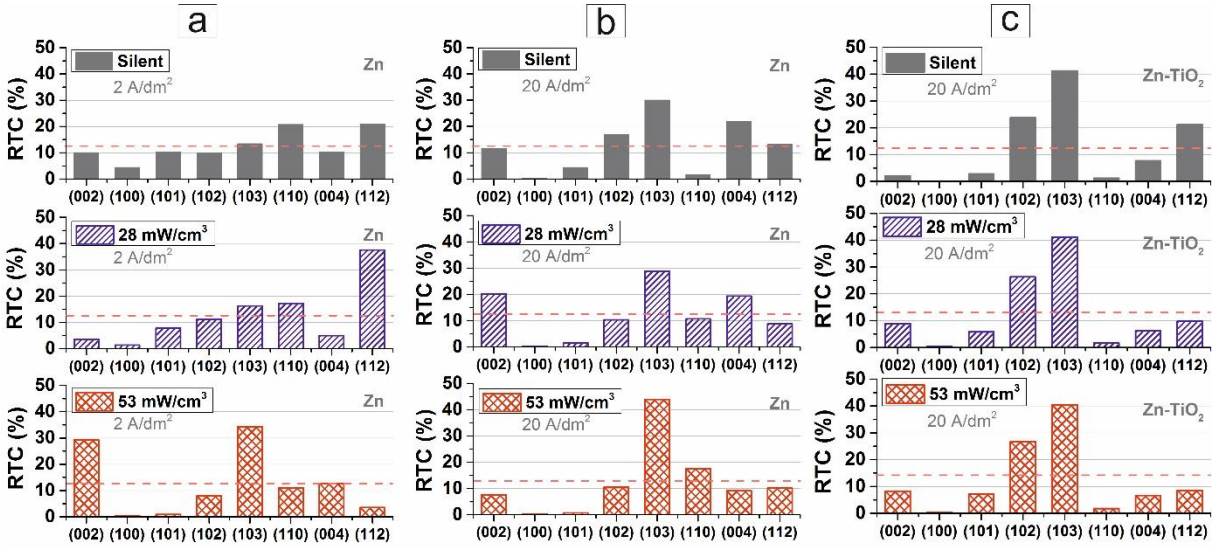

Figure 8 Influence of 38 kHz ultrasonic irradiation on the texture of electroplated Zn deposits: a) pristine Zn plated at 2 A/dm^2, b) pristine Zn plated at 20 A/dm^2 and c) Zn-TiO_2 plated at 20 A/dm^2. In all cases, the particle load was 15 g/L.

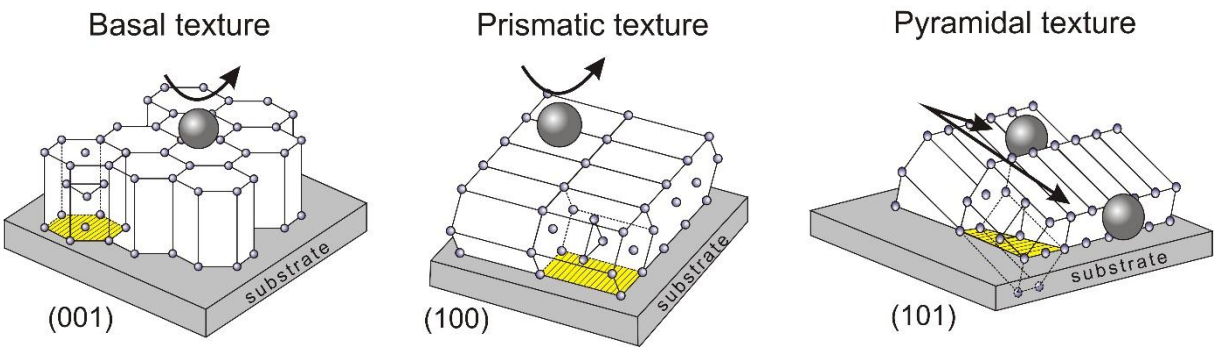

Figure 9 Schematic representation of the development of different textures during Zn electrodeposition

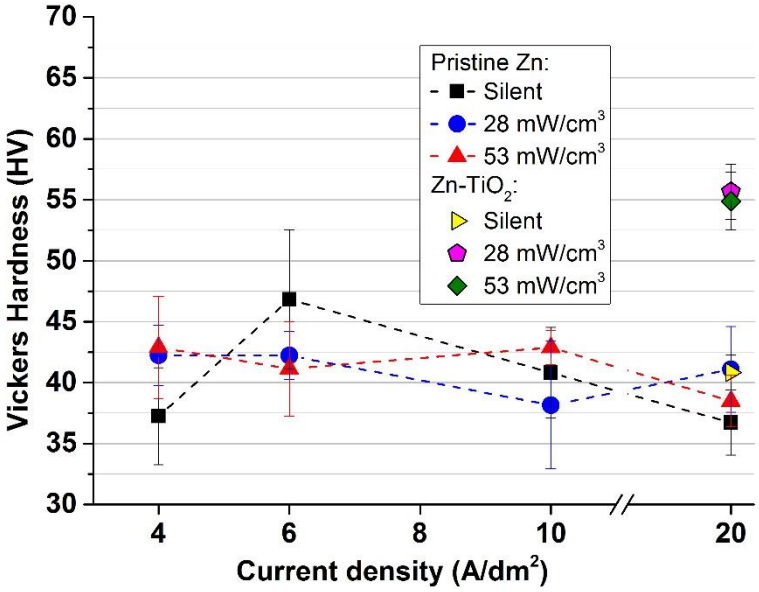

Figure 10 Influence of 38 kHz ultrasonic irradiation on the hardness of Zn and Zn-TiO_2 deposits plated at different current densities.

Tables

Table 1 Plating bath composition and electrodeposition parameters

a) Plating bath composition	
0.46 M $ZnCl_2$ (62.7 g/L) 2.75 M KCl (204.8 g/L) 0.40 M H_3BO_3 (25 g/L) TiO_2 P25 powder (15 g/L)	
b) Electrodeposition parameters	
pH	5.3
Temperature	room temperature
Substrate	low carbon steel disk (2.54 cm^2)
Rotation rate (RDE)	600 rpm
Anode	Zn plate (99.95% purity)
Current density	2, 4, 6, 10 and 20 A/dm^2
Charge density	36 C/cm^2

Table 2 Determination of the ultrasonic power input by calorimetry

Setting	Ultrasonic power input as:
US-bath (38 kHz)-ultrasonic nominal power	Power density (mW/cm^3)
70%	28
100%	53